





Investigation of Mechanical Properties in PVA Hydrogels Due to Cation Interactions Described by Reactive Forcefield Based Molecular Dynamics Simulations

JESSICA A. SCHULZE ¹, MALGORZATA KOWALIK,²
MUTIAN HUA,³ SHUWANG WU,³ YOUSIF ALSAID,³ XIMIN HE,³
and ADRI C.T. VAN DUIN ^{2,4}

1.—Department of Chemistry, Pennsylvania State University, University Park, PA 16802, USA. 2.—Department of Mechanical Engineering, Pennsylvania State University, University Park, PA 16802, USA. 3.—Department of Materials Science and Engineering, University of California, Los Angeles, CA 90095, USA. 4.—e-mail: acv13@psu.edu

Hydrogels are cross-linked networks containing water and are widely used in multiple fields due to their intrinsic softness and diffusive properties. One field of particular interest is in medical devices and tissue and organ engineering. Poly(vinyl alcohol) (PVA) is one common hydrogel where its mechanical properties can be changed by using different salt solutions, making it more appropriate for certain applications, such as artificial neuron tissue. In this study, we used the ReaxFF reactive forcefield to investigate PVA in lithium and potassium chloride. It was hypothesized that lithium might promote a proton transfer from the PVA hydroxyl groups, therefore inhibiting the PVA from forming hydrogen bonds with itself, yielding a weaker PVA hydrogel. Conversely, potassium would not promote a proton transfer, instead getting inside the PVA structure, allowing a higher density of hydrogen bonds to form, creating a stronger PVA hydrogel. We were able to show a proton transfer was favorable in the lithium case and unfavorable in the potassium case. This explains the differences in mechanical properties shown in experimental results and provides atomistic detail to motivate tunable mechanical properties in PVA hydrogels in various salt solutions.

INTRODUCTION

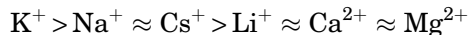
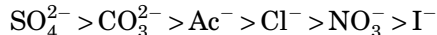
Hydrogels are a class of materials composed of hydrophilic cross-linked networks that have a high water content. Hydrogels have gained popularity and significant attention in research due to their wide array of applications in the fields of drug delivery,¹ neural probes,^{2,3} medical implants,^{4,5} energy storage,⁶ robotics,⁷ and coatings.⁸ In general, hydrogels have become favorable compared with traditional polymers because they tend to be biocompatible, biodegradable, non-toxic, and are able to transport water, ions, nutrients, and other biomolecules freely through their matrix.⁹ Natively,

hydrogels are soft and fragile due to their high water content (i.e., low solid content). However, in practice different applications require contrasting mechanical properties of these materials. For example, medical devices and robotics might require stiff hydrogels while drug delivery systems require soft hydrogels.¹⁰ Moreover, certain applications may require time-dependent mechanical properties that can change in situ over time, depending on external signals. One example of interest is using hydrogels in neuron probes. Sea cucumbers have the ability to change the toughness of their dermis rapidly. The ability to change toughness in the collagen fibrils in the sea cucumber's dermis has motivated research into changing the stiffness of other polymers based on an outside stimulus² such as water or temperature.¹¹ Changing a material's mechanical properties in situ would allow a neuron probe to start as a stiff

(Received March 1, 2022; accepted August 23, 2022)

material during insertion and then soften to mimic a neuron, which would prevent damage to the surrounding neurons.¹² This has motivated the research on gaining the ability to tune the mechanical properties of hydrogels.¹³

Poly(vinyl alcohol) (PVA) hydrogels are a representative class of hydrogels that show tunable mechanical properties in the presence of different ions. Wu et al., have been able to create an ultra-tough PVA hydrogel, with a toughness of $150 \pm 20 \text{ MJ m}^{-3}$, which has surpassed the mechanical properties of other regularly used synthetic polymers such as polydimethylsiloxane and rubber.¹⁴ In addition, they have realized tunability of PVA's mechanical properties over a toughness range of 0.0167 ± 0.003 to $150 \pm 20 \text{ MJ m}^{-3}$ and modulus range of 24 ± 2 to $2500 \pm 140 \text{ kPa}$.¹⁴ This has been accomplished by soaking PVA in various salt solutions motivated by the Hofmeister effect. The Hofmeister effect has been extensively researched for proteins and can predict the aggregation of proteins and polymers in the presence of salts.^{15,16} The difference in aggregation is correlated to the strength of the protein or polymer in the following order:



where sulfate salts produce the strongest and toughest polymers and magnesium, calcium, and lithium salts produce the weakest polymers.

To change the strength of the PVA, a soak-freeze method was employed by first dissolving the PVA in water completely and then freezing the solution. The frozen PVA solution was then placed in salt solutions of varying concentrations where the anions were paired with Na^+ and the cations were paired with Cl^- . This method guarantees that gelation of the PVA is directly from the salt solutions.¹⁴ Once the PVA starts to thaw, the structure is allowed to re-orient based on the salts, which may or may not result in gelation. Some salts will get inside the PVA structure causing the structure to collapse in on itself when the salts are removed, creating a stronger cross-linked network; this is known as the salting-out effect. Other salts will stay on the outside of the PVA and can break bonds when washed out, creating a weaker cross-linked network; this is known as the salting-in effect.^{16,17}

In this study, PVA soaked in lithium chloride and potassium chloride was investigated using ReaxFF for atomistic-scale simulations. Experimentally, it was found that potassium chloride made a stronger PVA hydrogel while the lithium chloride caused the PVA not to gel. These results follow the Hofmeister effect and the salting-in and -out phenomena. We hypothesized that lithium might promote a proton

exchange between the PVA and water, allowing the PVA to stay in the water and never gel. We also hypothesized that potassium will not promote proton transfer and instead move inside the PVA structure, causing a stiffer PVA gel. To explore these potential proton transfers, reactive molecular dynamics simulations, using the ReaxFF forcefield, were used to simulate PVA in potassium chloride and lithium chloride solutions.

The ReaxFF forcefield has shown to be accurate in similar systems, including proton transfers in the aqueous phase.^{18,19} Beyond proton transfer in just water, ReaxFF has been shown to accurately model proton transfer between organic systems in water.²⁰ Vashisth et al.²¹ showed that ReaxFF could be used to describe the cross-linking of polymers. Lastly, ReaxFF has been developed to accurately describe electrolyte-water systems.²² These previous results indicate that ReaxFF is an appropriate method to use in the PVA water system with potassium and lithium salts.

METHODS

To study PVA and its mechanical properties in the presence of potassium and lithium ions, the ReaxFF potential was used to perform reactive molecular dynamics (MD) simulations.²³ ReaxFF is mainly trained against density function theory data and uses a bond-order formalism. This allows ReaxFF the ability to form and break bonds while still enjoying the size and time-scale advantages of traditional MD simulations. This is accomplished by calculating the bond-order between every pair of atoms at every step of the simulation using the following equation:

$$\text{BO}'_{ij} = \exp \left[p_{bo,1} \left(\frac{r_{ij}}{r_0^\sigma} \right)^{p_{bo,2}} \right] + \exp \left[p_{bo,3} \left(\frac{r_{ij}}{r_0^\pi} \right)^{p_{bo,4}} \right] + \exp \left[p_{bo,5} \left(\frac{r_{ij}}{r_0^\pi} \right)^{p_{bo,6}} \right]. \quad (1)$$

The forcefield used for this study is a merge between the electrolyte-water forcefield developed by Fedkin et al.²² and the protein and peptide forcefield developed by Monti et al.²⁴ The Fedkin forcefield was trained using quantum mechanics and literature for bond lengths and bond angles of metal water clusters, water-binding energies, equations of state for metal oxide, hydroxide, and halide phases, and heats of formations for metal oxide and hydroxide condensed phases. The Monti forcefield was trained against quantum mechanics data for geometries, energies, valence bonds, torsional angles, and charge of multiple geometry conformations for each amino acid. To verify the forcefields' relevance for the PVA system, an NPT ensemble simulation at 300 K was performed on ten polymers, each consisting of ten PVA monomers, until the density converged (Fig. 1). The final density was 1.27 g/cm^3 which agrees with experimental results

of around 1.19–1.31 g/cm³.²⁵ The large experimental range comes from the PVA’s ability to have differing water content. Experimentally, the PVA was dissolved in water and then frozen. The PVA was then allowed to gel during the thawing process. Due to this, our model is meant to represent the PVA after thawing and therefore does not take into account specific cross-linking; instead the PVA polymers are allowed to interact with themselves during the duration of the simulation. These interactions include both long-range and chemical interactions from the ReaxFF method.

Because our hypothesis is partially based on proton transfer, we performed a study to analyze the reaction barrier associated with the transfer of a proton from the hydroxyl group of the PVA to water. A PVA decamer was created and an ion, either

potassium or lithium, was placed close to a PVA hydroxyl. Ten explicit water molecules were then placed surrounding the ion and PVA, providing local solvation. The proton from the PVA hydroxyl was subsequently forced to transfer to a water molecule as a result of the ion approaching the hydroxyl group. A bond restraint methodology was used based on the following equation²⁶

$$E_{\text{restraint}} = \text{Force}_1 * \left\{ 1.0 - \exp(\text{Force}_2 * (R_{ij} - R_{12})^2) \right\}. \quad (2)$$

In the case of potassium, 2 bond restraints were used: the first moved potassium closer to the hydroxyl oxygen and the second moved the proton away from the hydroxyl oxygen. In the case of lithium, 5 bond restraints were used: the first moved lithium closer to the hydroxyl oxygen, the second moved the proton away from the hydroxyl oxygen, the third moved the proton towards the accepting water oxygen, the fourth rotated the water to be in a position to accept the proton by moving a water hydrogen towards a hydroxyl oxygen next to the donating hydroxyl, and the fifth kept the water in that orientation while the proton transferred (Table I).

After the barrier study, proton transfer and ion movement relative to the PVA was investigated by looking at two systems: a PVA structure in a water salt solution and an ion substituted PVA structure in water. For the first system, the converged structure (Fig. 1) was placed in a water box surrounded by 1550 water molecules and either 50 potassium or lithium chloride salt molecules, which was enough ions to interact with the PVA during the simulation. An NVT ensemble was modeled for 1 ns at 300 K using a 0.5 fs time step. For the second system, a 50 monomer PVA chain was constructed and 50 of the hydroxyl protons were replaced with either lithium or potassium, representing an extreme case where proton transfer had already occurred. This system was then surrounded by 1000 water molecules and an NPT ensemble simulation was performed for 0.05 ns at 300 K using a 0.5 fs time step.

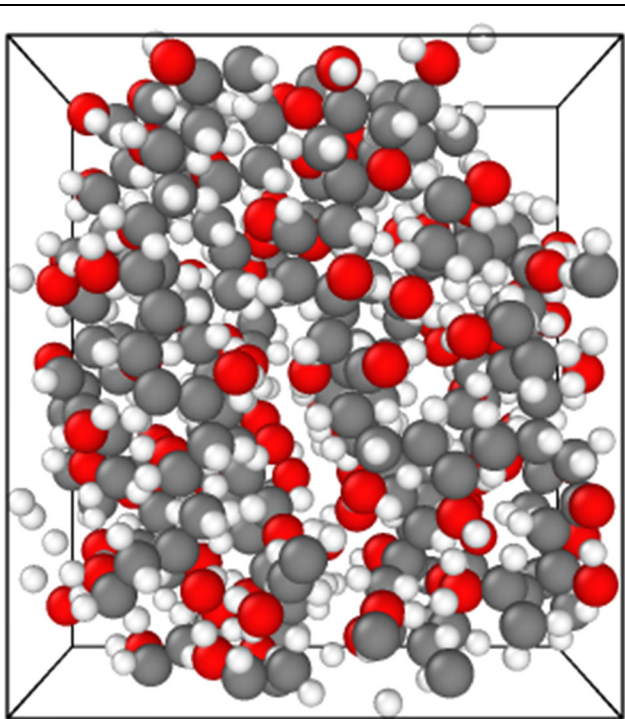


Fig. 1. Final structure of PVA with converged density of 1.27 g/cm³.

Table I. Bond restraint simulation parameters

Bond restraint	Force 1 (kcal/Å)	Force 2 (kcal/Å)	Change in distance (Å)	Steps
<i>Potassium</i>				
1	500.00	1.00	0.5	10,000
2	500.00	0.25	0.8	10,000
<i>Lithium</i>				
1	500.00	0.25	0.7	10,000
2	500.00	0.10	0.8	10,000
3	500.00	0.25	0.9	10,000
4	500.00	0.10	1.2	10,000
5	500.00	0.10	0.0	5000

Lastly, the mechanical properties were explored using a compression and expansion simulation. The final structures of the 1 ns NVT simulation for both potassium and lithium were taken and the total volume of the system was compressed and expanded to 50% of the original volume in all directions over 100,000 steps. Only the volume and energy data necessary to calculate bulk modulus was used for analysis purposes.

RESULTS AND DISCUSSION

To determine whether a proton transfer occurs in the potassium and lithium case, the energy from the bond restraint simulations were analyzed. The potassium simulation had a higher barrier height than the lithium simulation (Fig. 2a, b, and c). This implies that if a proton transfer occurs in the potassium case, it could be reversed. However, in the lithium case, if a proton transfer occurs, the proton transfer may not be reversible.

To further investigate our hypothesis, water and salt ions were added and surrounded the PVA system. A radial distribution function (RDF) and coordination number plot was created between the

ions and the center of mass of the PVA for every 0.25 ns. The RDF plot shows the density of ions from the center of mass of the PVA as a function of distance, and the coordination plot shows the number of ions at a certain distance away from the center of mass of the PVA. We averaged the RDF and coordination plots every 0.25 ns to show how the system evolves with time. The RDF and coordination plots show that both potassium and lithium get closer to the PVA as the simulation progresses (Fig. 3c, d, e, and f). In the case of potassium, between 10 and 15 Å, the potassium ions do get closer to the PVA as time progresses compared with the lithium case. The PVA has a radius of around 11 Å, so the change in potassium ion distance in the 10- to 15-Å range could imply potassium is getting close enough to get inside the PVA structure. When potassium gets inside the PVA and is subsequently washed out, it will create a more crosslinked PVA structure. In the case of lithium, when lithium gets closer to the PVA, lithium facilitates a proton transfer instead of getting inside the PVA structure (Table II). At the start of the simulation, all of the ions were present in the chloride salts. After 1 ns, all of the potassium ions were in the water phase

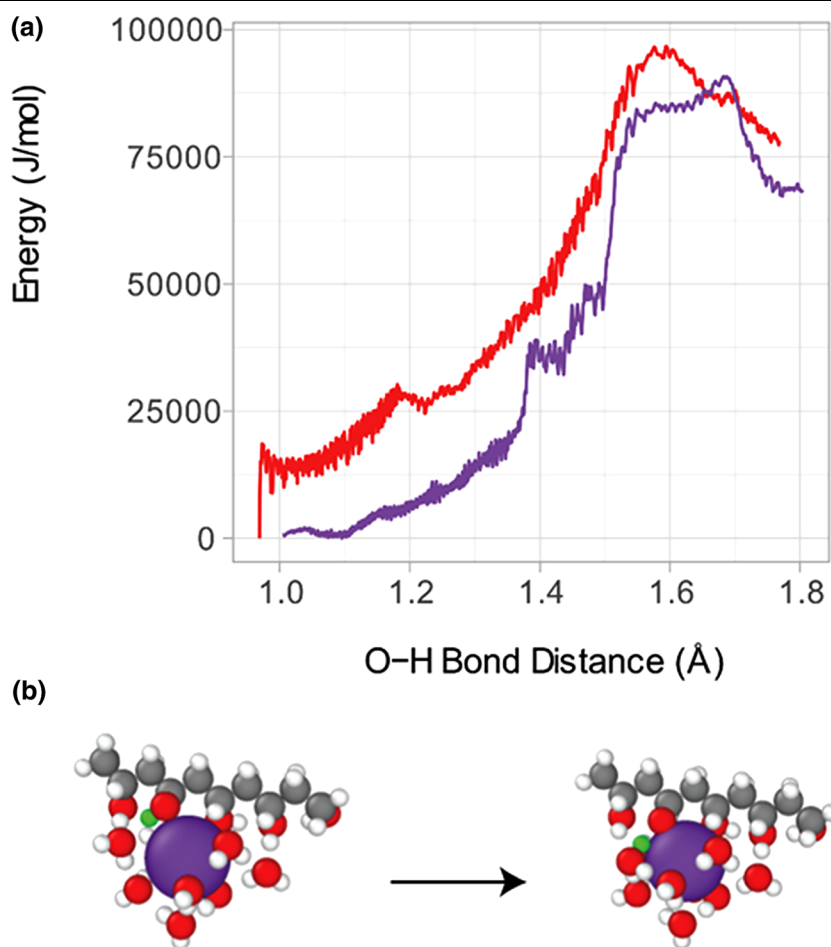


Fig. 2. (a) Total energy versus reaction coordinate associated with the O-H bond distance using a bond restraint methodology. (b) Initial and final configuration for a proton (green) exchange with potassium or lithium (purple) (Color figure online).

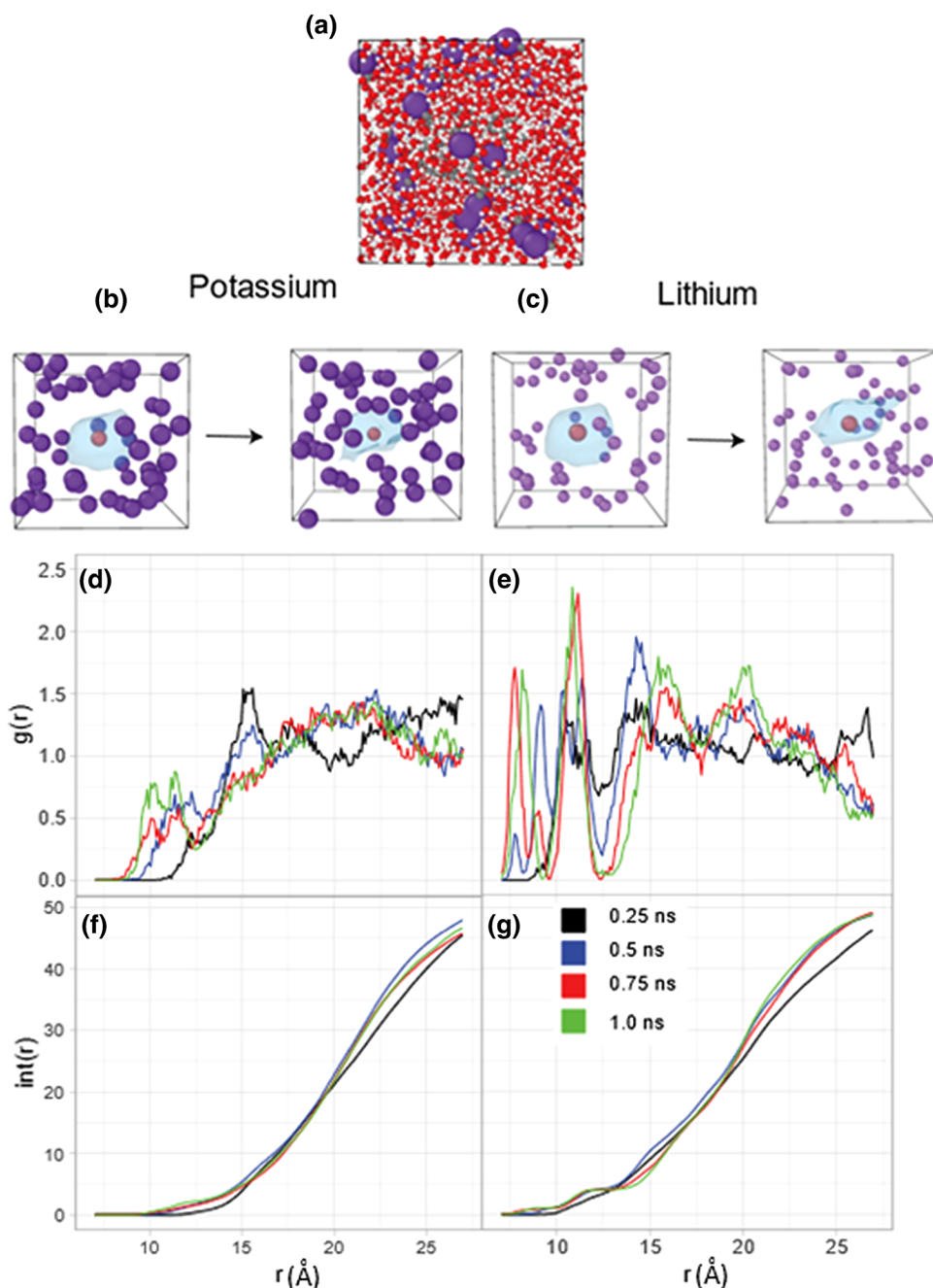


Fig. 3. (a) Full simulation cell with PVA, water, and potassium or lithium chloride. (b) Initial and final structure of ions with potassium (purple), PVA center of mass (orange) and surface of PVA (blue). (c) Initial and final structure of ions with lithium (purple), PVA center of mass (orange) and surface of PVA (blue). (d) RDF for potassium and center of mass of PVA every 0.25 ns. (e) RDF for lithium and center of mass of PVA every 0.25 ns. (f) Coordination number of potassium and center of mass of PVA every 0.25 ns. (g) Coordination number of lithium and center of mass of PVA every 0.25 ns (Color figure online).

while seven of the lithium atoms were associated with the PVA and 43 lithium atoms were associated with the water (Table II). Association was determined by ReaxFF taking the connection tables and then using a bond order cutoff to perform a fragment analysis. When a proton transfer occurs, the PVA is able to dissolve back into the water phase, creating a weaker structure. This suggests that lithium is able to promote a proton transfer while

potassium stays in solution as an ion, thus supporting our hypothesis. Comparing these results with experiments, it is observed that PVA soaked in potassium chloride does indeed create a stronger network than in lithium chloride based on stress-strain curves of PVA soaked in 3 M potassium and lithium salt solutions (Fig. 4).¹⁴

An extreme case where 50 of the protons on the PVA were already substituted with the ions was analyzed to see whether the proton transfer was reversible (Fig. 5a). At the start of the simulation all of the ions were associated with the PVA. By the end

of the simulation, only one potassium ion was still associated with the PVA while 49 lithium ions were still associated with the PVA. The one lithium ion not associated with the PVA was associated with a water molecule. For potassium, one ion was associ-

Table II. Number of associations between potassium and lithium with the PVA at the initial and final configurations, and water associations and ions at the end of the simulation

Type of association	Number of associations with potassium	Number of associations with lithium
Initial PVA	0	0
Final PVA	0	7
Water	0	43
Ion	50	0

Association was determined by ReaxFF taking the connection tables and then using a bond order cutoff to perform a fragment analysis.

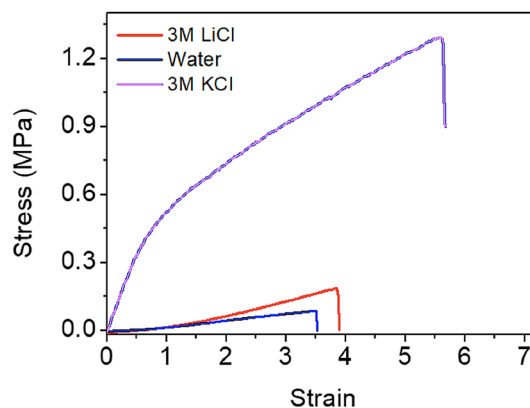


Fig. 4. Experimental stress versus strain curves for PVA in water and 3 M lithium and potassium chloride ¹⁴.

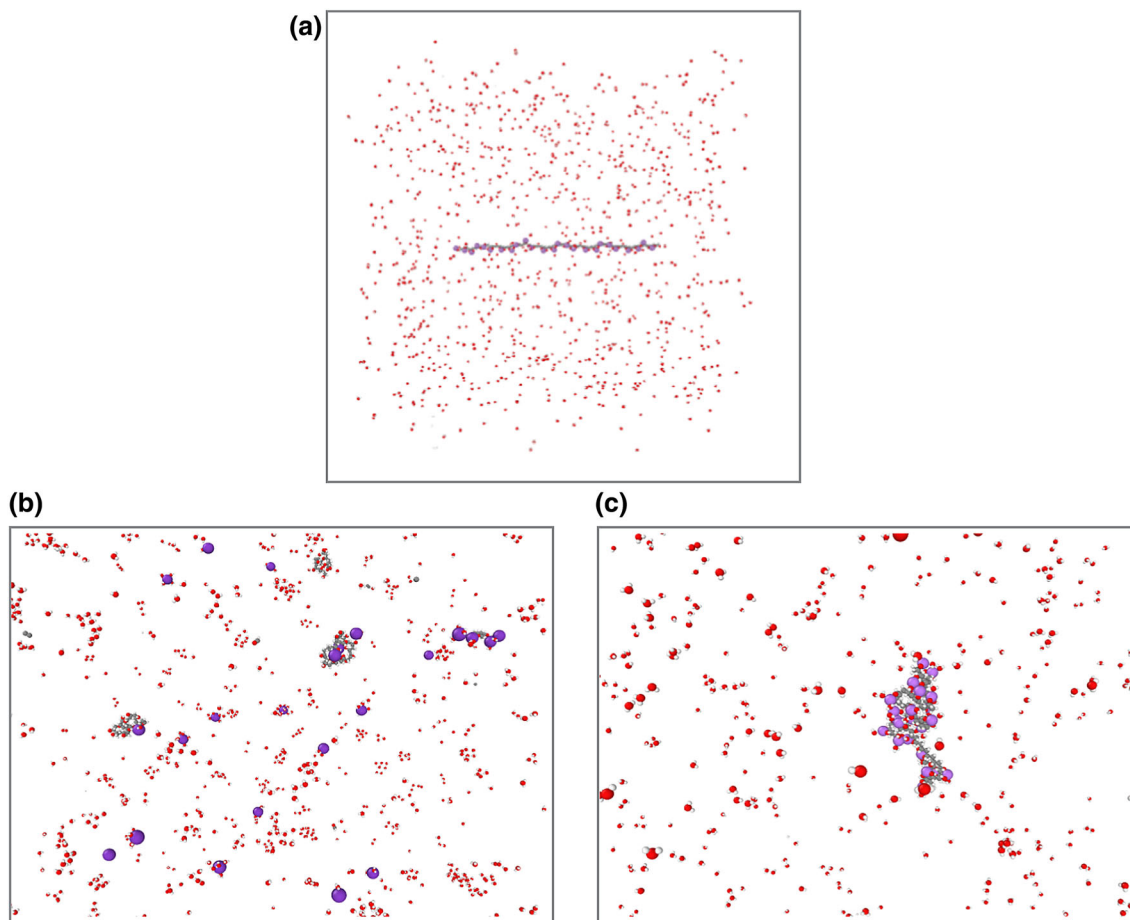


Fig. 5. (a) Initial PVA with 50 hydroxyls substituted by an ion and surrounded by 1000 water molecules. (b) Final structure for potassium coordinated PVA. (c) Final structure for lithium coordinated PVA.

ated with a hydroxyl, one ion was associated with water, and the remaining 47 atoms were ions in solution (Table III). When the potassium ions went back into solution, it broke apart the PVA carbon backbone, forming small PVA clusters (Fig. 5b) compared with lithium, which stayed associated with the PVA, where the PVA started to fold in on itself (Fig. 5c). This implies that once a proton transfer occurs, it is reversible in the potassium case and irreversible in the lithium case.

Finally, the mechanical properties were analyzed by comparing the potential energy curves for PVA in water, and 3 M lithium and potassium solutions in compression and expansion simulations. Due to the computational constraints on our system size, multiple cross-linking was not seen in the simulations, unlike in experiments. However, looking at the potential energy (Fig. 6) the simulations still show potassium with the highest mechanical response,

followed by lithium, then water. Looking at snapshots of the simulations (Fig. 6), lithium is able to preferentially coordinate with the PVA chains, unlike potassium. This is verified by looking at the RDF between the ions and PVA (Fig. 6). Experimentally calculated bulk modulus results also show that PVA soaked in potassium chloride will have the highest bulk modulus, then lithium chloride, then water (Fig. 7).¹⁴ Both the computational and experimental results follow the trend that potassium has the highest mechanical response, then lithium, then water, which can be explained by the Hofmeister effect.¹⁴

CONCLUSION

Hydrogels have gained prominence in research fields due to their biocompatibility, including biodegradable, non-toxic, and matrix properties that

Table III. Number of associations between potassium and lithium with the PVA at the initial and final configurations, water and hydroxyl associations, and ions at the end of the simulation

Type of association	Number of associations with potassium	Number of associations with lithium
Initial PVA	50	50
Final PVA	1	49
Water	1	1
Hydroxide	1	0
Ion	47	0

Association was determined by ReaxFF taking the connection tables and then using a bond order cutoff to perform a fragment analysis.

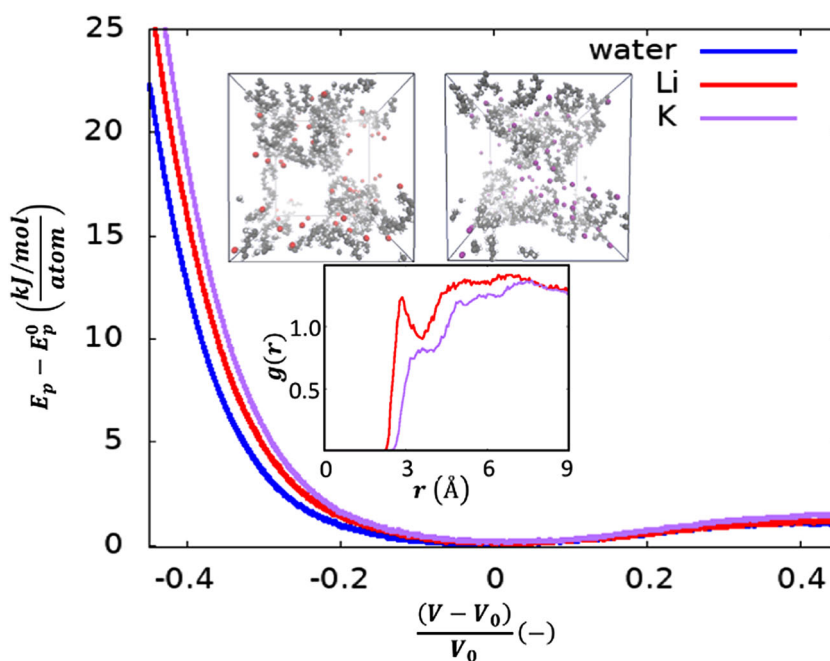


Fig. 6. Potential energy versus relative change in volume of compression and expansion simulations from experimental results for PVA in water, 3 M lithium solution, and 3 M potassium solution. Snapshots of PVA surrounded by lithium (red) and potassium (purple) are shown as insets. The RDF graph also confirms the coordination of lithium with the PVA chains compared with potassium (Color figure online).

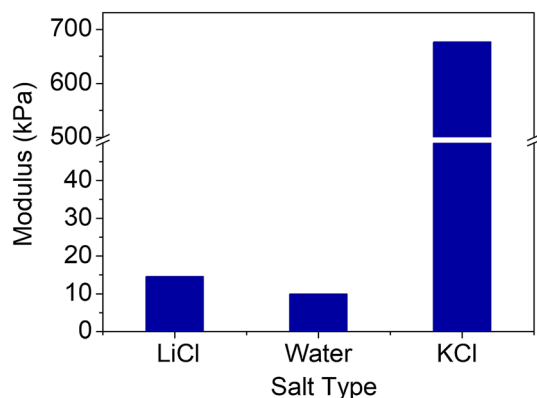


Fig. 7. Experimental bulk modulus results for lithium chloride, water, and potassium chloride ¹⁴.

allow diffusion through the material, and their use in a multitude of applications in particular medical devices and tissue and organ engineering. However, due to their high water content, hydrogels are inherently soft materials, causing problems in applications such as robotics and medical devices that require more stiff materials. PVA hydrogels have been shown to have tunable mechanical properties by soaking the PVA in salt solutions, based on the Hofmeister effect. We show that lithium promotes a proton transfer between PVA and water while potassium does not, and instead moves inside the PVA structure. This explains the observation that PVA does not gel in the presence of lithium but does gel in the presence of potassium. A mechanical response test confirmed that potassium will make the stiffest PVA, followed by lithium and pure water. These simulations have been used to explain why potassium ions create a stiffer hydrogel and why lithium causes the PVA to dissolve back into solution; our simulations indicate that this is due to potassium being able to get inside the PVA structure and because lithium cations are likely to promote a proton transfer. This hypothesis can be applied to hypothesize whether a cationic salt will create a stiffer or weaker PVA hydrogel and motivate which experiments to perform based on the desired result. Additional computational studies are in progress to determine why different anionic salt solutions have different effects on PVA hydrogels' mechanical properties.

ACKNOWLEDGEMENTS

Jessica A. Schulze acknowledges support and training provided by the Computational Materials Education and Training (CoMET) NSF Research Traineeship (Grant No. DGE-1449785). Mutian Hua, Yousif Alsaïd, and Ximin He acknowledge support provided by the NSF CAREER award 1724526, Air Force Office of Scientific Research award (FA9550-17-1-0311), and the Office of Naval Research Award (N000141712117).

CONFLICT OF INTEREST

The authors declare that they have no known competing financial interests or personal relationships that could have appeared to influence the work reported in this paper.

REFERENCES

1. J. Li and D.J. Mooney, *Nat. Rev. Mater.* 1, 16071 (2016).
2. J.R. Capadona, K. Shanmuganathan, K.D.J. Tyler, S.J. Rowan, and C. Weder, *Science* 319, 1370 (2008).
3. S.K. Seidlits, Z.Z. Khaing, R.R. Petersen, J.D. Nickels, J.E. Vanscoy, J.B. Shear, and C.E. Schmidt, *Biomaterials* 31, 3930 (2010).
4. Y. Liu, J. Liu, S. Chen, L. Ting, K. Yeongin, N. Simiao, H. Wang, X. Wang, A.M. Foudeh, J.B.H. Tok, and B. Zhenan, *Nat. Biomed. Eng. Lond.* 3, 58 (2019).
5. K.Y. Lee and D.J. Mooney, *Chem. Rev.* 101, 1869 (2001).
6. Y. Huang, M. Zhong, F. Shi, X. Liu, Z. Tang, Y. Wang, Y. Huang, H. Hou, X. Xie, and C. Zhi, *Angew. Chem. Int. Ed.* 56, 9141 (2017).
7. H. Yuk, S. Lin, C. Ma, M. Takaffoli, N.X. Fang, and X. Zhao, *Nat. Commun.* 8, 14230 (2017).
8. X. Yao, J. Liu, C. Yang, X. Yang, J. Wei, Y. Xia, X. Gong, and Z. Suo, *Adv. Mater.* 31, 1903062 (2019).
9. J.M. Korde and B. Kandasubramanian, *Ind. Eng. Chem. Res.* 49, 9709 (2019).
10. H. Fan and J.P. Gong, *Macromolecules* 53, 2769 (2020).
11. Y. Qiu, E. Askounis, F. Guan, Z. Peng, W. Xiao, Q. Pei, and A.C.S. Appl. Polym. Mater. 2, 2008 (2020).
12. J.P. Harris, A.E. Hess, S.J. Rowan, C. Weder, C.A. Zorman, D.J. Tyler, and J.R. Capadona, *J. Neural Eng.* 8, 056014 (2014).
13. X. Zhao, *Soft Matter* 10, 672 (2014).
14. S. Wu, M. Hua, Y. Alsaïd, Y. Du, Y. Ma, Y. Zhao, C. Lo, C. Wang, D. Wu, B. Yao, J. Strzalka, H. Zhou, X. Zhu, and X. He, *Adv. Mater.* 33, e2007829 (2021).
15. P. Jungwirth and P.S. Cremer, *Nat. Chem.* 6, 261 (2014).
16. S.Z. Moghaddam and E. Thormann, *J. Colloid Interface Sci.* 555, 615 (2019).
17. R. Sadeghi and F. Jahani, *J. Phys. Chem. B* 116, 5234 (2012).
18. A.C.T. van Duin, Z. Chenyu, J. Kaushik, B. Vyascheslav, and W.A. Goddard, *Comput. Catal.* 14, 223 (2013).
19. W. Zhang and A.C.T. van Duin, *J. Phys. Chem. B* 121, 6021 (2017).
20. O. Rahaman, A.C.T. van Duin, W.A. Goodard, and D.J. Doren, *J. Phys. Chem. B* 115, 249 (2011).
21. A. Vashisth, C. Ashraf, W. Zhang, C.E. Bakis, and A.C.T. van Duin, *J. Phys. Chem. A* 112, 6633 (2018).
22. M.V. Fedkin, Y.K. Shin, N. Dasgupta, J. Yeon, W. Zhang, D. van Duin, A.C.T. van Duin, K. Mori, A. Fujiwara, M. Machida, H. Nakamura, and M. Okumura, *J. Phys. Chem. A* 123, 2125 (2019).
23. T.P. Senftle, S. Hong, M.M. Islam, S.B. Kylasa, Y. Zheng, Y.K. Shin, C. Junkermeier, R. Engel-Herbert, M.J. Janik, H.M. Aktulga, T. Verstraelen, A. Grama, and A.C.T. van Duin, *NPJ Comput. Mater.* 2, 15011 (2016).
24. S. Monti, A. Corozzi, P. Fristrup, K.L. Joshi, Y.K. Shin, P. Oelschlaeger, A.C.T. van Duin, and V. Barone, *Phys. Chem. Chem. Phys.* 15, 15062 (2013).
25. NIH, Polyvinyl alcohol. <https://pubchem.ncbi.nlm.nih.gov/source/hsdb/1038#section=Density>. Accessed 22 June 2021.
26. A.C.T. van Duin, ReaxFF User Manual. <https://www.scm.com/wp-content/uploads/ReaxFF-users-manual-2002.pdf>. Accessed 22 June 2021.

Publisher's Note Springer Nature remains neutral with regard to jurisdictional claims in published maps and institutional affiliations.